30. *Aftershocks of Imaichi Earthquake Observed at Nishi-oashi Station.*

By Syun'itiro OMOTE,

Earthquake Research Institute.

(Read Sep. 17, 1950—Received Sep. 20, 1950).

1. Introduction.

The Imaichi earthquake that shook the northern part of the Kwanto District on Dec. 26, 1949, was followed by a fairly large number of aftershocks. For the purpose of observing these aftershocks a temporary network of seismic stations was established soon after the main shock. These stations were Imaichi, Nikko, Funyu, Kanuma and Nishi-oashi, and at the last named station the author installed two seismometers of horizontal components and one of vertical component and carried out the registration of aftershocks in terms of three components of seismographs. In the former studies on aftershocks, such as those of Tango,[1] Tottori,[2] Fukui[3] and even of this Imaichi earthquake,[4] the location of foci was made entirely by the so-called "difference time method"[5] of three or four stations. The distribution of the foci of Imaichi aftershocks is discussed in another article[4] in this same bulletin. The number of shocks whose foci were located and reported on in that article in the period from Dec. 29 to Jan. 8 was 21 or so. In the case of the present observation, however, highly sensitive horizontal motion seismometers were installed at Nishi-oashi Station, and by the aid of a vertical motion seismometer, we were able to locate the foci of some one hundred aftershocks from the data obtained at the single station, Nishi-oashi, the result of which study will form the subject of the present article.

2. The Observations at Nishi-oashi Station.

The observation of afterocks at Nishi-oashi Station began on Dec. 31 and continued until Jan. 6 of the next year. The instrumental constants of the seismographs used then are listed in Table I.

1) N. NASU, *Jour. Fac. Sci. Tokyo. Univ.*, 3 (1929), 29.
2) S. OMOTE, *Bull. Earthq. Res. Inst.*, 22 (1944), 33.
3) S. OMOTE, *Rep. Fukui Earthq.*, (1950, Tokyo), 37.
4) EARTHQ. RES. INST., *Bull. Earthq. Res. Inst.*, 28 (1950), 387.
5) BULLEN, "Introduction to the Theory of Seismology." 1924, (London).

Table I.

Type	Component	Period sec.	Weight kg.	Geomtrical magnification	Damping ratio
Displacement seismograph	Horizontal	1.0	50	235	8 : 1
Acceleration seismograph	Vertical	0.1	25	165	8 : 1

As soon as observations were started at Nishi-oashi we noticed that shocks of short P—S times were recorded frequently here and that these near shocks had energy large enough to give distinct beginnings to the records of the first motions. Some examples of these seismograms will be reproduced in the Plate. Daily numbers of shocks recorded at the Nishi-oashi Station and the frequency distribution of P—S times of these aftershocks will be seen in Figs. 1 and 2.

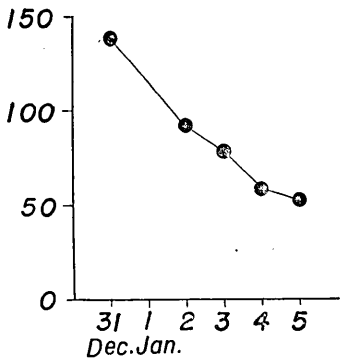

Fig. 1. Daily numbers of recorded shocks at Nishi-oashi.

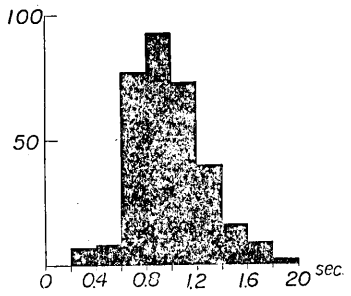

Fig. 2. Frequency diagram of P—S times.

The amplitudes of the first maximums of the respective shocks were read from the seismograms and are tabulated in Table II. The direction of the epicenter from the station was obtained by compounding the amplitudes of the first waves of P on the E—W and N—S component seismograms as vectors. The focal distance was computed from the P—S intervals observed at the station, the Omori constant k being given the value k=7.1 according to the result computed in the study of Imaichi aftershocks by the difference time method. In order to examine the accuracy of the epicenters determined by this single station method, we compared them with the epicenters of the same aftershocks determined by the difference time method. In Fig. 3 the foci of seven shocks obtained by these two different methods are compared. Open circles in Fig. 3 represent the foci located by the difference time method, and black dots those located by the single station method. Figures attached to

Table II.

Earthq. No.	Commencement time. d h m	Trace amplitude of initial motion. (× 1/20 mm) E-W	N-S	U-D	P—S time sec.	Period of initial motion. T_V sec.	T_H sec.	α	β	θ
1	31 12 16	− 1.0	+ 3.5	− 9.0	0.8	0.12	0.36	0.08	0.59	1°40′
2	12 33	+ 6.5	+ 13.0	− 6.0	1.2	0.04	0.12	0.55	0.84	40°55′
3	13 02	− 3.5	− 1.0	− 1.0	0.9	0.08	0.24	0.22	0.72	19°20′
4	15 31	− 5.0	− 8.5	+ 4.0	1.4	0.05	0.15	0.43	0.83	34°46′
5	15 49	+ 9.0	+ 9.0	− 11.5	1.7	0.08	0.24	0.22	0.72	10°06′
6	16 04	+ 10.0	+ 6.0	− 10.5	0.9	0.08	0.24	0.22	0.72	10°29′
7	17 52	+ 9.0	+ 1.0	− 11.0	1.0	0.08	0.24	0.22	0.72	8°07′
8	18 57	+ 18.0	+ 15.0	− 2.5	1.1	0.11	0.33	0.12	0.62	51°11′
9	22 25	− 3.0	− 2.0	− 1.0	1.1	0.04	0.12	0.55	0.84	53°21′
10	23 08	+ 2.0	− 4.0	− 2.0	0.9	0.06	0.18	0.37	0.78	33°30′
11	23 43	+ 8.0	+ 7.0	− 18.5	0.8	0.08	0.24	0.22	0.72	5°29′
12	1 0 11	+ 2.0	− 1.5	− 1.5	0.7	0.08	0.24	0.22	0.72	15°28′
13	0 13	+ 17.0	− 19.5	− 13.0		0.06	0.18	0.37	0.78	30°16′
14	0 34	− 6.5	− 6.5	+ 5.0	1.2	0.06	0.18	0.37	0.78	28°21′
15	0 37	+ 19.0	+ 3.5	− 7.0	1.4	0.08	0.24	0.22	0.72	24°42′
16	0 51	+ 2.0	+ 3.5	− 2.0	1.2	0.06	0.18	0.37	0.78	30°21′
17	0 54	− 4.5	− 7.5	+ 7.5	1.3	0.04	0.12	0.55	0.84	22°35′
18	1 07	+ 3.5	− 1.5	+ 5.0	1.3	0.08	0.24	0.22	0.72	7°14′
19	1 11	− 3.0	− 2.0	+ 2.5	1.2	0.04	0.12	0.55	0.84	27°03′
20	1 11	+ 2.0	− 6.0	+ 7.5	1.3	0.04	0.12	0.55	0.84	16°22′
21	16 35	− 2.5	− 3.0	+ 4.5	1.2	0.06	0.18	0.37	0.78	14°08′
22	16 50	− 2.0	− 1.5	+ 3.0	1.0	0.02	0.08	0.67	0.88	18°54′
23	17 08	+ 2.5	+ 2.0	− 2.0	0.8	0.06	0.18	0.37	0.78	25°06′
24	17 54	− 2.5	− 2.5	+ 5.5	0.7	0.04	0.12	0.55	0.84	12°42′
25	18 15	+ 2.0	+ 1.5	− 3.5	0.9	0.08	0.24	0.22	0.72	6°49′
26	19 08	+ 20.0	+ 13.0	− 7.0	0.9	0.10	0.30	0.13	0.65	2°24′
27	20 18	− 4.0	+ 3.0	− 3.0	0.9	0.04	0.12	0.55	0.84	30°35′
28	22 00	− 2.0	− 2.0	+ 2.0	1.2	0.04	0.12	0.55	0.84	26°22′
29	22 17	− 3.5	− 1.5	+ 6.0	1.1	0.08	0.24	0.22	0.72	6°02′
30	2 0 19	− 6.0	− 2.0	− 94.0		0.12	0.36	0.08	0.59	2°48′
31	1 37	+352.0	+440.0	−112.0	1.6	0.10	0.13	0.05		19°10′
32	2 07	+ 2.0	+ 1.0	− 3.5	0.9	0.04	0.12	0.55	0.84	12°29′
33	2 14	− 3.0	− 3.0	+ 2.0	1.5	0.08	0.24	0.22	0.72	19°49′
34	3 38	− 1.5	− 1.0	+ 2.0	1.2	0.01	0.03	0.83	0.95	23°03′
35	3 50	− 2.0	− 2.0	+ 2.0	1.2	0.06	0.18	0.37	0.78	22°19′

(to be continued)

(continued)

Ear. thq. No.	Commencement time. d h m	Trace amplitude of initial motion. (× 1/20 mm) E-W	N-S	U-D	P—S time sec.	Period of initial motion. T_V sec.	T_H sec.	α	β	θ
36	3 57	− 2.0	− 2.5	− 0.5	1.2	0.04	0.12	0.55	0.84	10°38′
37	10 50	+ 7.0	0	− 3.0	1.0	0.09	0.27	0.17	0.68	17°21′
38	11 10	+ 1.5	− 2.0	− 2.0	0.4	0.04	0.12	0.55	0.84	24°12′
39	12 14	− 1.0	− 1.5	+ 4.0	0.6	0.04	0.12	0.55	0.84	9°04′
40	13 43	− 2.0	+ 1.5	− 1.0	0.8	0.08	0.24	0.22	0.72	11°59′
41	15 11	+ 16.0	+ 6.0	− 11.5	1.0	0.04	0.12	0.55	0.84	27°47′
42	15 50	− 6.0	− 6.0	+ 9.0	1.1	0.08	0.24	0.22	0.72	8°52′
43	16 30	+ 2.5	+ 1.0	− 2.0	0.8	0.06	0.18	0.37	0.78	21°31′
44	18 43	− 5.5	− 7.5	+ 3.0	1.4	0.07	0.23	0.30	0.73	27°55′
45	18 52	+ 1.0	+ 2.5	− 1.0	1.7	0.06	0.18	0.37	0.78	38°30′
46	19 23	+ 24.0	+ 8.5	− 10.5	1.3	0.08	0.24	0.22	0.72	33°30′
47	20 02	+ 2.0	− 1.0	+ 1.0	1.2	0.06	0.18	0.37	0.78	18°10′
48	20 32	+ 23.5	0	− 10.0	1.3	0.08	0.24	0.22	0.72	21°26′
49	20 54	+ 2.0	+ 3.5	+ 1.0	1.4	0.04	0.12	0.55	0.84	57°31′
50	21 18	− 7.0	− 6.5	+ 5.0	1.2	0.10	0.30	0.13	0.65	11°42′
51	23 53	− 12.0	− 42.0	+ 21.0		0.08	0.24	0.22	0.72	19°15′
52	3 6 15	− 1.5	− 4.0	+ 3.5	1.3	0.04	0.12	0.55	0.84	23°34′
53	7 27	− 4.0	− 3.0	+ 6.5	0.8	0.06	0.18	0.37	0.78	12°43′
54	8 27	+ 15.0	+ 10.0	− 7.5	0.6	0.08	0.24	0.22	0.72	21°50′
55	9 33	− 1.5	− 2.0	+ 3.0	1.0	0.04	0.12	0.55	0.84	16°24′
56	12 22	+ 4.0	+ 1.5	− 5.0	0.9	0.06	0.18	0.37	0.78	14°09′
57	15 47	−101.5	− 10.3	+ 55.0	1.4	0.10	0.30	0.13	0.65	20°40′
58	15 49	− 3.5	− 3.0	+ 2.0	1.7	0.07	0.21	0.29	0.76	26°06′
59	15 52	− 6.0	− 9.0	+ 3.0	1.5	0.06	0.18	0.37	0.78	47°17′
60	17 14	+ 19.5	− 30.0	− 10.0	1.0	0.10	0.30	0.13	0.65	20°14′
61	21 44	+ 2.0	+ 2.0	− 3.0	0.8	0.04	0.12	0.55	0.84	18°16′
62	22 22	+ 2.5	+ 1.5	− 4.0	0.9	0.04	0.12	0.55	0.84	14°25′
63	22 34	− 1.5	− 31.0	− 12.0	0.8	0.06	0.18	0.37	0.78	21°05′
64	22 35	+ 3.0	+ 1.5	− 3.0	0.9	0.05	0.15	0.46	0.83	18°45′
65	22 35	− 2.0	− 5.0	− 2.0	0.8	0.04	0.12	0.55	0.84	42°02′
66	4 8 56	− 2.5	− 7.0	+ 2.0	1.4	0.10	0.30	0.13	0.65	24°29′
67	9 06	+ 3.5	+ 1.5	+ 11.0	0.9	0.04	0.12	0.55	0.84	9°50′
68	9 20	+ 3.0	+ 3.0	− 4.5	0.9	0.06	0.18	0.37	0.78	15°26′
69	13 16	+ 4.5	+ 3.5	− 6.0	0.9	0.08	0.24	0.22	0.72	8°24′
70	13 46	− 4.0	− 6.0	+ 1.5	1.5	0.10	0.30	0.13	0.65	28°00′

(to be continued)

(Continued)

Earthq. No.	Commencement time. d h m	Trace amplitude of initial motion. (× 1/20 mm) E-W	N-S	U-D	P—S time sec.	Period of initial motion. Tv sec.	TH sec.	α	β	θ
71	4 16 18	− 5.0	+ 9.0	+ 6.0	1.1	0.08	0.24	0.22	0.72	15°43′
72	18 02	− 1.0	− 5.5	+ 3.0	1.1	0.10	0.30	0.13	0.65	11°21′
73	20 03	+ 7.0	+ 3.5	− 6.5	1.0	0.08	0.24	0.22	0.72	11°13′
74	22 11	+ 9.0	+ 10.0	− 8.5	0.7	0.08	0.24	0.22	0.72	14°57′
75	22 33	+ 6.0	− 14.0	− 6.5	1.1	0.04	0.12	0.55	0.84	39°51′
76	22 54	− 5.0	− 5.0	+ 7.0	1.3	0.04	0.12	0.55	0.84	21°13′
77	23 22	+ 6.0	+ 1.5	− 6.5	1.2	0.06	0.18	0.37	0.78	15°32′
78	23 28	− 3.7	− 4.5	+ 5.0	0.9	0.07	0.23	0.30	0.73	11°21′
79	5 2 46	+ 9.5	+ 2.0	− 9.0	0.7	0.06	0.18	0.37	0.78	17°42′
80	2 54	+ 3.0	+ 4.0	− 4.5	1.1	0.06	0.18	0.37	0.78	17°57′
81	3 46	− 1.0	− 4.0	+ 1.5	1.6	0.08	0.24	0.22	0.72	23°57′
82	12 11	+ 6.0	− 24.5	− 9.0	1.2	0.16	0.49	0.05	0.47	9°11′
83	12 59	− 1.5	− 4.5	+ 3.5	1.0	0.04	0.12	0.55	0.84	20°23′
84	13 35	+ 18.5	− 44.0	− 9.0	0.8	0.14	0.42	0.07	0.53	20°49′
85	13 54	+ 30.0	− 40.5	− 12.5	1.1	0.12	0.36	0.08	0.59	16°27′
86	16 41	+ 7.5	+ 3.5	− 4.5	0.9	0.08	0.24	0.22	0.72	17°09′
87	21 14	− 1.5	− 3.5	+ 2.0	0.8	0.04	0.12	0.55	0.84	34°03′
88	22 17	+ 2.0	− 8.0	− 3.0	1.4	0.06	0.18	0.37	0.78	38°50′
89	23 52	+ 2.0	− 7.5	− 2.0	0.9	0.04	0.12	0.55	0.84	55°37′
90	23 54	− 2.5	− 3.0	+ 4.0	0.3	0.06	0.18	0.37	0.78	16°05′
91	6 7 15	+ 3.0	+ 2.5	− 5.5	0.3	0.08	0.24	0.22	0.72	7°26′
92	7 55	− 2.0	− 1.0	+ 1.5	0.6	0.04	0.12	0.55	0.84	27°58′
93	7 56	+ 2.0	+ 1.5	+ 1.0	0.4	0.06	0.18	0.37	0.78	36°19′
94	8 06	+ 4.5	+ 3.5	− 3.0	1.0	0.06	0.18	0.37	0.78	29°06′
95	8 33	− 1.5	− 4.5	+ 1.0	1.9	0.12	0.41	0.22	0.55	59°10′

the circles refer to the earthquake numbers in Table II. It will be seen that, with respect to some aftershocks, considerable differences have resulted in the focal distances of the same shocks. This is because in Fig. 3 the focus located from single station data was assumed to exist on the surface of the earth. For our present purpose, then, only the azimuths of foci should be compared. The difference in azimuth is tabulated in Table III, and the mean deviation in azimuth was calculated as $12°.3 \pm 4°.5$.

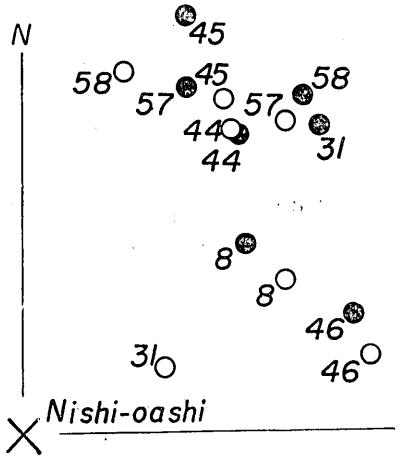

Fig. 3. Comparison of epicenters.
○; epicenter by difference time method.
●; epicenter by single station method.

Table III. Azimuth of epicenter determined by
A ; the difference time method,
B ; the single station method.

Earthq. No.	46	8	31	57	45	44	58
A (from N to E)	78.5	60.2	66.0	40.3	32.0	35.0	16.5
B („)	71.0	50.2	45.0	26.5	21.5	36 2	40.0
Difference	7.5	10.0	21.0	14.3	10.5	-1.2	—

3. The Epicenters Located by the Data at a Single Station.

Through the investigations explained in the preceding paragraphs we were convinced that fairly reliable locations of epicenters were to be obtained from the data at a single station. Referring to Table II we were able to locate the foci of the shocks, assuming that focal depths of these shocks were all zero kilometer. Geographic distribution of these foci is shown in Fig. 4. For the sake of comparison the map of epicenters of aftershocks during the same period, prepared by the difference time method, is reproduced in Fig. 5. These two maps closely resemble each other. As seen in Fig. 4, the result obtained by the single station method also shows that large numbers of aftershocks have occurred in the region to the northeast of Nishi-oashi Station.

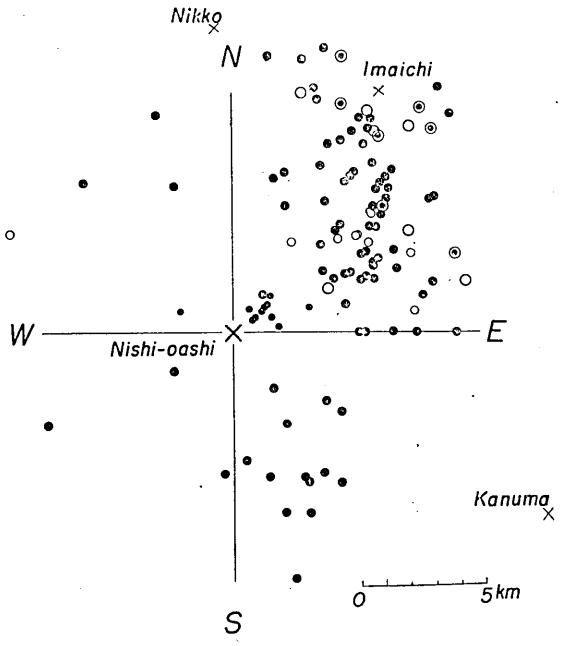

Fig. 4. Distribution of epicenters of shocks from Dec. 31 to Jan. 6 determined by the single station method.

Now when the area is divided into four quadrants by E—W and N—S lines intersecting at Nishi-oashi Station, some points of difference will be noticed between these two maps:

1) Not a small number of foci are seen located in the quadrant IV or the southeast quadrant by the single station method, while only a few shocks were located in this quadrant by the difference time method. The frequency curves of the P—S durations at Kanuma Station show that a considerable number of earthquakes of short P—S duration times (less than 2 seconds) are observed there, and it will be reasonable to consider that although small shocks had certainly occurred in this quadrant, the foci of such shocks were so distant

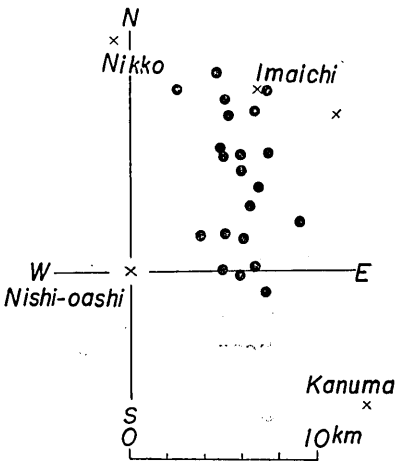

Fig. 5. Distribution of epicenters of shocks from Dec. 31 to Jan. 6 determined by the differnce time method. (After T. Hagiwara)

from Nikko or Imaichi Stations that the seismometers in these stations failed to catch them.

2) According to the result due to the difference time method, not a single epicenter has been located in the quadrants II and III. Nevertheless, our single station method reveals the existence of seven shocks with their foci in these quadrants. With respect to these seven shocks careful examinations have been carried out with the original seismograms, so that it may safely be said that the location of these shocks in the two quadrants is to be relied upon.

3) In the quadrant III, the most distant area from the active region, at least three shocks—admittedly a very small number—are seen to have occurred during this period.

4. The Depth of Focus.

As Nishi-oashi Station was equipped with a vertical motion seismometer besides two components of horizontal motion seismometers, we tried to compute the true angle of incidence of P waves in order to acquire some knowledge concerning the depth of the foci of aftershocks. As will be seen in Table I the free oscillation period of the vertical motion seismometer was adjusted at 0.1 second, so that the amplitude in their seismograms represents the acceleration of the motion of the earth, while that of the horizontal motion seismometers was adjusted at 1.0 second, so that in their seismograms will be recorded the displacement of the earth movement whose period is about 0.3 sec. Such being the case, the use of direct trace amplitude of seismograms does not readily make possible the quantitative determination of the incident angle. Since true earth amplitude is to be obtained by twice integrating[6] the recorded seismograms, we also subjected some of the records of vertical seismometers to these procedures and obtained the results given in Fig. 6. Displacement curves, however, are inevitably affected by the shifting of zero lines, so that, from this method of calculation, the

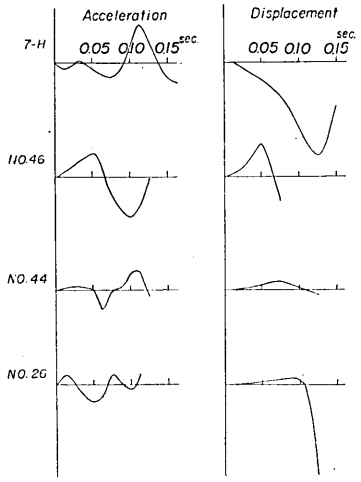

Fig. 6.
Acceleration: Original acceleration seismogram.
Displacement: Disp'acement curve computed from the acceleration seismogram.

6) T. HAGIWARA, *Bull. Earthq. Res. Inst.*, 13 (1935), 138.

accurate value of the amplitude of the first motion is not to be measured. In order to eliminate this inaccuracy we made use of the results of calculation carried out by Dr. C. Tsuboi.[7] He computed the motion of a pendulum when it was exposed to the external vibration of the forms:

$$\begin{cases} t<0 & f(t)=0 \\ t\geqq 0 & f(t)=a\sin\omega t \end{cases} \qquad \cdots\cdots(1)$$

or

$$\begin{cases} t<0 & f(t)=0 \\ t\geqq 0 & f(t)=2\sin t-\sin 2t\,. \end{cases} \qquad \cdots\cdots(2)$$

He also drew a graph that shows how much the recorded first maximum amplitude is reduced according to the fluctuation of the ratios of apparent period of the recorded initial motion to that of the seismographs. The apparent initial periods of the vertical motion were read from the seismograms and tabulated in column T_V in Table II, while the apparent initial periods of the horizontal motion were computed by T. Suzuki's method[8] and shown in column T_H in the same Table. In our present study of Nishi-oashi records the initial motion of aftershocks had a sudden commencement as will be seen in the seismograms in the Plate, and so the equation (1) was made use of for computation. The coefficients for the correction of the initial apparent amplitudes on vertical and horizontal seismometers are seen in Table II, columns α and β. The apparent incident angle $\bar{i}$ will be calculated by

$$\tan\bar{i}=\frac{A_H}{A_V}=\frac{a_H}{a_V}\,\frac{\alpha}{\beta}\,\frac{V_H}{V_V}$$

where A_H and A_V are the true initial amplitudes of horizontal and vertical earth displacements, a_H and a_V the initial amplitudes of the observed motions, and V_H and V_V the magnification coefficients of the instruments. The true angle of incidence computed from these is shown in the last column in Table II. In computing the true incident angle, the value of $V/_V$, the ratio of the velocities of longitudinal and transversal waves, was assumed to be 1.7 after T. Matuzawa[9].

In Fig. 7 are shown the frequency diagrams of the incident angle due to every ten degrees. According to the data obtained by T. Suzuki[10] at Tokyo and Mitaka some time ago, almost all the angles of incidence of seismic waves were found to be less than ten degrees, or in other words almost all seismic

7) C. TSUBOI, *Bull. Earthq. Res. Inst.*, 12 (1934), 426.
8) T. SUZUKI, *Bull. Earthq. Res. Inst.*, 12 (1934), 16.
9) T. MATUZAWA, *Bull. Earthq. Res. Inst.*, 6 (1920), 177.
10) T. SUZUKI, *Bull. Earthq. Res. Inst.*, 10 (1932), 518.

waves had nearly vertical directions. Contrary to this, in the case of Nishi-oashi observation, the majority of seismic waves had an incident angle from 10 to 30 degrees, only a small number of waves having angles less than ten degrees. Apparently this is because the geological conditions near the earth's surface in Nishi-oashi region are totally different from those in the Tokyo district, none of the soft layer of quaternary loam existing to disturb the wave paths to a remarkable extent.

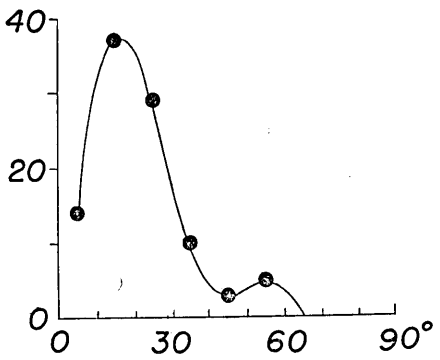

Fig. 7. Frequency diagram of incident angles.

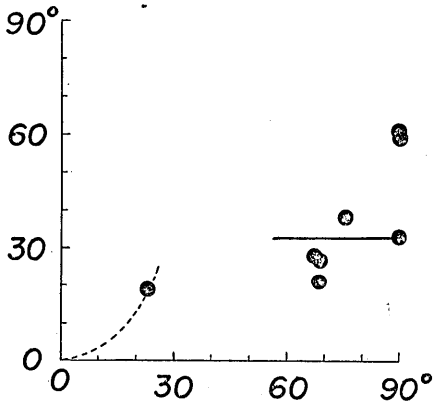

Fig. 8. Incident angles computed by the single station method (ordinate) as related to those computed by difference time method (abscissa).

The result of the study of aftershocks by the difference time method enables us to measure the angle formed by the wave path—namely the line from the focus to the station—and vertical line that passes through the station. This angle is contrasted in Fig. 8 with the incident angle computed by our single station method. As seen in the figure, the incident angle of the shock No. 5 is almost equal to the angle obtained by the difference time method, but when the incident angles calculated by the difference time method were 60~80 degrees, the angles computed by Nishi-oashi Station were about thirty degrees. The incident angles of four shocks that had very shallow origins will be contrasted with each other in Table IV. As seen in the table, though the incident angles observed at Nishi-oashi Station were fairly large with respect to the shocks whose epicentral distances were less than ten kilometers, shocks with longer epicentral distances had rather small incident angles.

In explanation of these facts we are led to suppose a discontinuity within the earth at the depth of a few kilometers. Supposing a P wave that started at some point near the discontinuous surface traveled along the boundary of

Table IV. Comparison of the incident angles computed by different methods.

θ: Incident angle computed by single station method.
i: Incident angle computed by difference time method.
Δ: Epicentral distance.

Earthq. No.	θ	i	Δ	Earthq. No.	θ	i	Δ
			km				km
8	51.2°	90.0°	8.1	46	33.5°	90.0°	9.4
31	19.2°	23.0°	4.2	57	20.7°	68.5°	10.8
44	27.9°	67.7°	9.8	58	26.1°	68.5°	9.8
45	38.5°	75.5°	10.3	95	59.2°	90.0°	12.0

the discontinuity and was refracted back to the observation station, such a wave will have the angle of incidence of 35 degrees, provided the second layer had a velocity of 7 km/s or so. Now as it is known that the focal depth of the majority of aftershocks is about five kilometers, if the above assumption is made, it will be understood that the peaks of the frequency curves of angles of incidence are seen at about 10~30 degrees. In the next place, assuming the depth of the discontinuity was less than 2.5 kilometers, the refracted waves will arrive at the station earlier than the direct waves, provided the origin of the shock was placed at the surface of the earth and the distance from the origin to the station was greater than 12 km. If such is the case it is possible that distant shocks will have smaller incident angles of the first wave than near ones.

It will be difficult to obtain positive geological evidences to support this view of subsurface structure, but it may not be altogether impossible to assume a discontinuous surface within the granitic layer.

As to the shocks with very small angles of incidence, we calculated their focal depths. If we use without any modification the values of the angles of incidence given in the last column, the epicentral distances will become too small. We therefore assumed that these small angles contained an error of 5 degrees. On this assumption the epicentral distances of these shocks were calculated and plotted in Fig. 4 by small dots. Small open circles show the location of foci when the shocks represented by the corresponding small dots are supposed to have the depth of zero meter.

5. The Distribution of First Impulsions.

As the foci of aftershocks have been determined in the preceding paragraphs, we will consider next the problem of the distribution of first impulsions. In this case too, as we did in the case of Fukui aftershocks,[11] we assume that

11) S. OMOTE, *Bull. Earthq. Res. Inst.*, 28 (1950), 312.

a shock occurred at point 0 in Fig 9 and observation of it was made at positions designated by circles in the same figure. In reality we have one observation station and 95 foci distributed all around it, but now we assume that a shock occurred at the point 0 and was observed at 95 stations distributed all around it, the observation of first impulsions of P wave being carried out at the respective stations. Fig. 9 was drawn upon these assumptions, and the directions of the arrows indicate whether the first impulsions were directed toward or away from the epicenter, and the length of an arrow represents the ratio of the first horizontal amplitude of P wave to the amplitude of the largest motion, and a circle represents the sense of the first impulsion of the vertical component of the shock, open circles in it showing the downward motion and black ones the upward motion. From Fig. 9 it appears difficult to draw lines that bound the regions of the initial upward and downward motions. We notice, however, that all points in the northwest quadrant represent the initial downward motions, and in the southeast the majority of the points represent the upward, while in the southwest quadrant downward and upward signs are mixed together. Some similarities may be seen if we compare this map with the map showing the distribution of the first impulsions of the main shock.[12] In preparing Fig. 9, it is assumed that all the aftershocks took place with the same mechanism and at the same focal depth. These assumptions, however, involve exceptionnal conditions and are in reality almost impossible.

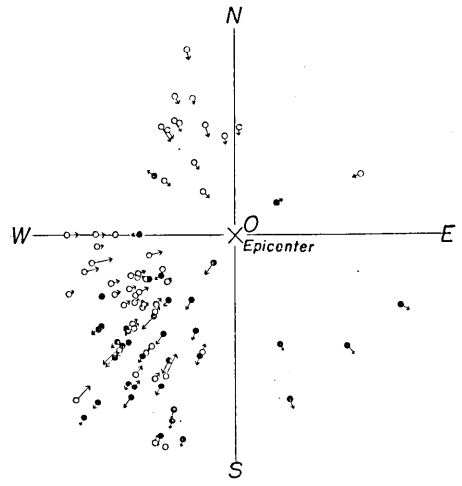

Fig. 9. Distribution of the direction of the initial motions.
Open circle; first condensational wave, black circle; first rarefactional wave.

6. Résumé.

In concluding these reports, the results obtained will be summarized as follows:—

12) *loc. cit.*, 4).

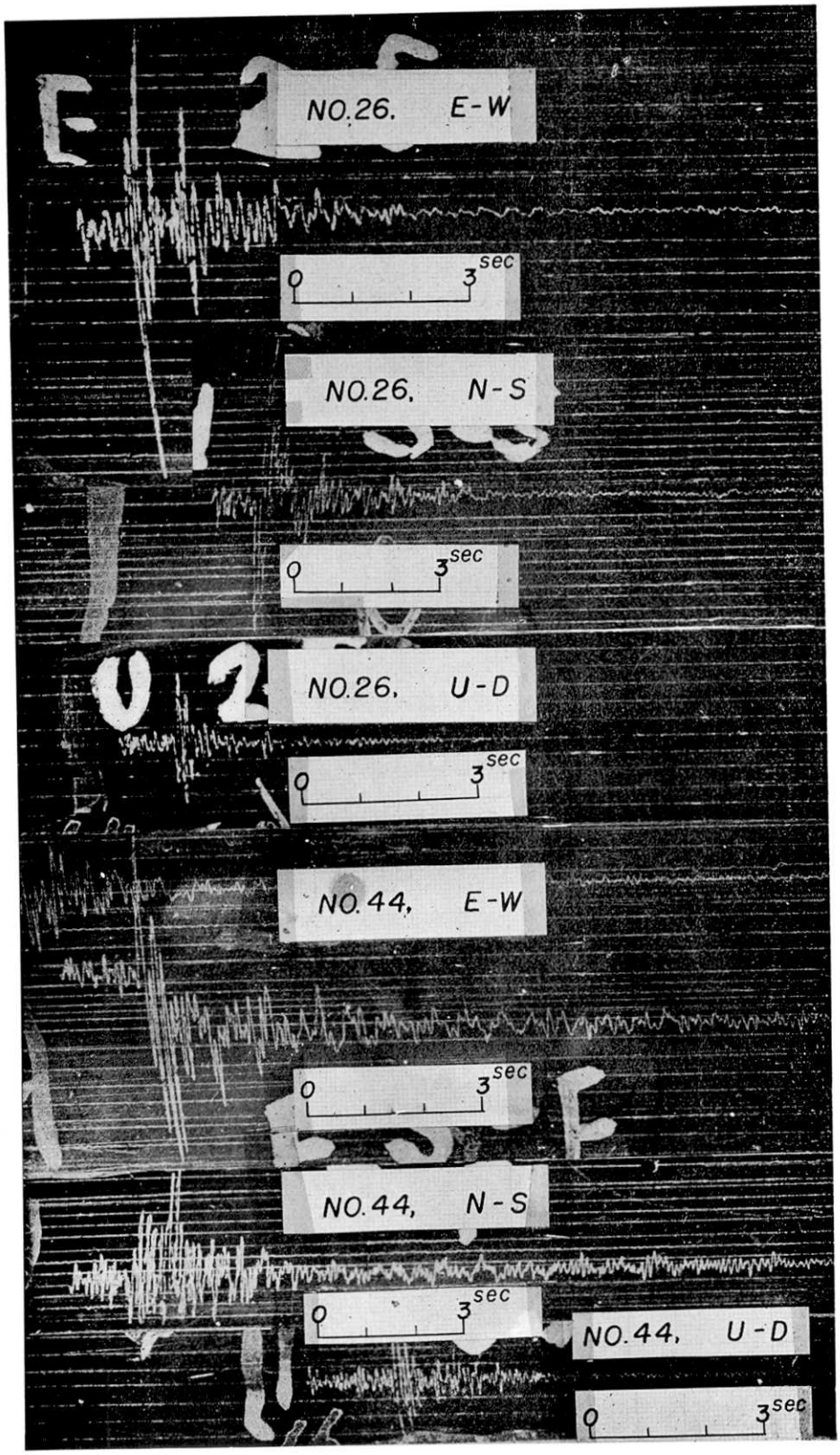

Fig. 10. a. Seismograms obtained at Nishi-oashi Station.

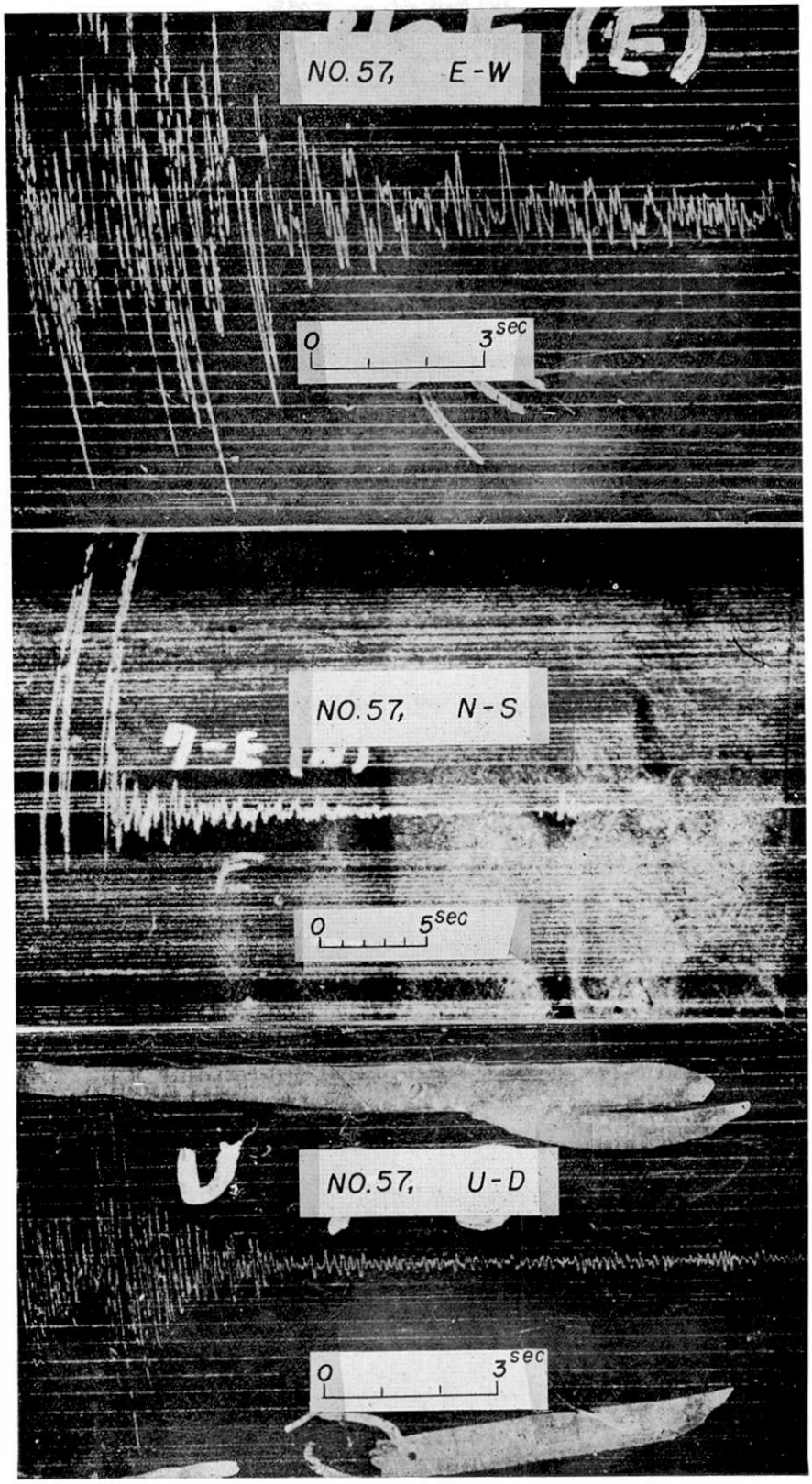

Fig. 10. b. Seismograms obtained at Nishi-oashi Station.

(1) Some 95 foci of Imaichi aftershocks were located by the data obtained at the single station, Nishi-oashi, which had three components of seismographs at its desposal.

(2) Epicenters of these aftershocks were mainly concentrated in the area bounded by a triangle whose apices were Nishi-oashi, Imaichi and Nikko, and this fact was in good accord with the result obtained by the difference time method.

(3) Occurrence of shocks, though small in number, in the northwest and southwest quadrants was confirmed.

(4) The incident angle of the first P wave was calculated. In this, as the vertical motion seismometer had the free oscillation period of 0.1 sec., Tsuboi's method was made use of for the purpose of determining the true initial amplitude of the vertical component.

(5) The majority of shocks had incident angles of about 10°～30° and the assumption of the existence of a discontinuity surface with a slightly bigger velocity within the earth was found to provide favourable explanation to it. The depth of this discontinuity will not be greater than 2.5 km.

(6) With respect to these shocks with small incident angles the depth of foci and the epicentral distance were calculated.

(7) Some observations were made regarding the distribution of the first impulsions of aftershocks.

In conclusion the author wishes to express his hearty thanks to Professor T. Hagiwara for his valuable advices. A part of the expense of this study was defrayed from the Scientific Research Fund of the Department of Education.

---

30. 西大芦村で觀測された今市地震の余震

地震研究所　表　俊一郎

今市地震の余震觀測は今市，日光，船生，鹿沼及西大芦で行はれそれらの結果より求められた余震の震央分布については別に報告されてゐる．筆者は西大芦に於て水平動の微動計2台，上下動の加速度計1台を用ひ三成分觀測を行つた．微動計はしばしば針が外れ觀測は困難であつたが初動は極めて明瞭な記錄が得られたので之等の記錄より一點觀測による震央を求めた結果，4點觀測による震央の位置と azimuth にして 10° 位の差違を生ずるが，その結果はだ分信賴するに足るものであることが解つた．求められた震央は大部分西大芦の北東，日光今市西大芦を結ぶ三角形の中で發生しその他西大芦鹿沼間にも可なりの地震が發生したことが知られた．入射角を計算するにあたつては坪井教授の求められた初動の型を用ひてもとめた結果 10°～30° の入射角をもつものが最も多いことが知られた．又極めて淺い地震についても震央距離の大きいものの方が入射角が反つて小となることが知られ之等より地下數粁の所に一つの層を考へうれば之等の現象を說明するのに極めて好都合であることをのべた．